Impulse approximation in nuclear pion production reactions: Absence of a one-body operator

Daniel R. Bolton and Gerald A. Miller
Department of Physics, University of Washington, Seattle, Washington 98195-1560, USA
(Received 16 February 2011; revised manuscript received 9 May 2011; published 24 June 2011)

The impulse approximation of pion production reactions is studied by developing a relativistic formalism, consistent with that used to define the nucleon-nucleon potential. For plane wave initial states we find that the usual one-body (1B) expression $\mathcal{O}_{1B}$ is replaced by $\mathcal{O}_{2B} = -iK(m_\pi/2)\mathcal{O}_{1B}/m_\pi$, where $K(m_\pi/2)$ is the sum of all irreducible contributions to nucleon-nucleon scattering with energy transfer of $m_\pi/2$. We show that $\mathcal{O}_{2B} \approx \mathcal{O}_{1B}$ for plane wave initial states. For distorted waves, we find that the usual operator is replaced with a sum of two-body operators that are well approximated by the operator $\mathcal{O}_{2B}$. Our new formalism solves the (previously ignored) problem of energy transfer forbidding a one-body impulse operator. Using a purely one pion exchange deuteron, the net result is that the impulse amplitude for $np \to d\pi^0$ at threshold is enhanced by a factor of approximately two. This amplitude is added to the larger "rescattering" amplitude and, although experimental data remain in disagreement, the theoretical prediction of the threshold cross section is brought closer to (and in agreement with) the data.

DOI: 10.1103/PhysRevC.83.064003 PACS number(s): 25.40.Ve, 12.39.Fe, 25.10.+s, 21.30.Fe

I. INTRODUCTION

It has been known for several decades that the chiral symmetry of the strong nuclear force in the $m_q \to 0$ limit can be exploited to formulate an effective field theory using hadrons as fundamental degrees of freedom rather than quarks and gluons [1–3]. This theory, generically called chiral perturbation theory (ChPT), is widely used in both the mesonic and the $A = 1$ sectors. Much effort is being put into the application of ChPT to the $A = 2$ sector, with success at low energies [4–6]. The frontier of this program is the pion production threshold, where the relative momentum between colliding nucleons is $p = \sqrt{m_\pi m_N}$. Pion production is also interesting in its own right as it provides a window into three nucleon forces [7] and can be used to extract information about charge symmetry breaking [8,9].

Being an effective theory, ChPT contains an infinite number of interactions organized in terms of importance according to a power counting scheme with an expansion parameter of m_π/Λ_χ where $\Lambda_\chi \approx m_N$ is the scale at which the theory ceases to become valid. For the problem of pion production one finds an additional parameter $\chi \equiv p/m_N = m_\pi/p \approx 0.4$. The fact that this parameter is large provides a significant challenge and a reorganized counting scheme was proposed in Ref. [10].

For a nice review of the history of meson production see Ref. [11]. The present study considers the specific reaction $NN \to d\pi$ (the two reactions $pp \to d\pi^+$ and $np \to d\pi^0$ are related by isospin symmetry), with the pion in an s wave. Furthermore, we are focusing on the contribution of a specific diagram, the impulse approximation (IA), also known as "direct" production, in which the produced pion does not interact at all with the spectator nucleon. We would like to be clear that pion rescattering, not the IA, is known to be the largest contribution to the total cross section [12]. The $\Delta(1232)$ resonance is also known to contribute significantly to this observable. Our motivation for the present study is to obtain increased precision in the total cross section calculation and to prepare for future application to other observables to which the IA contributes, such as p-wave pion production.

An additional challenge in the calculation of pion production is the presence of strongly interacting initial/final states. Because NN potentials are only now becoming reliable at such high energies, one typically employs a hybrid calculation in which a kernel is calculated perturbatively from ChPT and then convolved with wave functions calculated from phenomenological potentials. Recently this method has come under question for the IA [13,14]. Ideally, one would like to derive the correct method from a relativistic formalism that cleanly separates effects in wave functions from those appearing in the kernel.

Consider the IA contribution to $NN \to d\pi$ in the plane wave (PW) approximation where initial state interactions are neglected (see Fig. 1). The amplitude for such a process has been estimated to go like $\mathcal{M}^{IA} \sim \frac{m_\pi}{m_N}\boldsymbol{\sigma}\cdot\mathbf{p}_1\phi(p) \sim \frac{m_\pi}{m_N}\sqrt{m_N m_\pi}\phi(p)$, where $\phi(p)$ is the bound state wave function, evaluated in momentum space. The suppression by $m_\pi^{3/2}$ was noted in Ref. [10], which also included an analysis that a more detailed treatment of the power counting based on including initial and final state interactions introduces a power of $1/m_\pi$ via an energy denominator such that the amplitude varies as $\sqrt{m_\pi}$. Nevertheless, we see directly an explicit $m_\pi^{3/2}$ times $\phi(\sqrt{m\ m_\pi}\ )$.

In the physical region where $m_\pi = 140$ MeV, the wave function falls as a power of momentum greater than unity. For small values of relative momentum, the deuteron wave function also falls more rapidly than an inverse power of its argument. If one takes m_π to be small, the deuteron remains weakly bound [15,16] and therefore its momentum wave function will also fall rapidly in the chiral limit. Thus the power counting can only be considered a very rough estimate. If we follow [10], the impulse term is a leading order term, but the deuteron wave function is quite small for physical values of p and there is also a substantial cancellation between the deuteron s and d states. Thus this term's contribution to the cross section [12] is small and there is a contradiction between power counting expectations and realistic calculations.

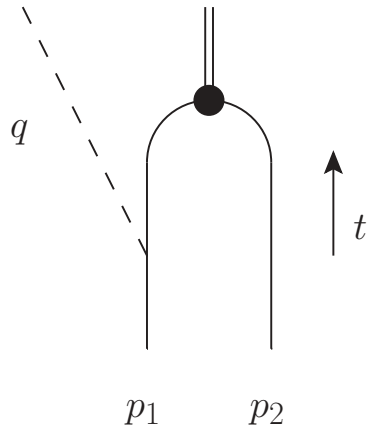

FIG. 1. Impulse approximation without initial state interactions. Solid lines represent nucleons, dashed lines represent pions, and double solid lines represent a deuteron.

This contradiction was also discussed at length in Ref. [13] where the authors introduced "wave function corrections" as a possible solution. This proposal included one-pion exchange (OPE) with an energy transfer of $m_\pi/2$ in the impulse kernel, but then subtracted off a similar diagram with static OPE in order to prevent double counting. The result depended strongly on the treatment of the intermediate off-shell nucleon propagator and no definitive conclusion was reached. This present work is intended to settle the debate regarding the inclusion of OPE in the impulse approximation. We demonstrate by starting from a consistent relativistic formalism that nonstatic OPE is to be included with no subtraction necessary; the impulse amplitude that should be used is given in Eq. (29). Furthermore, we show that the traditional approach of using a one-body kernel is correct only in the absence of initial state interactions.

In Sec. II we review aspects of the Bethe-Salpeter (BS) formalism for the two-nucleon problem. Section III presents the $N \to N\pi$ operator and Sec. IV shows that for plane wave $NN \to d\pi$, the traditional impulse approximation is approximately valid. Next, Sec. V considers the full distorted-wave amplitude by calculating the corresponding loop diagram, including the effects of the nonzero time components of the momenta of the exchanged mesons. In this section we are able to interpret the distorted-wave amplitude as a sum of two-body operators. We demonstrate the new formalism by explicitly evaluating s-wave $NN \to d\pi$ amplitudes at threshold. To aid the flow of the arguments, approximations made in this section are verified to be subleading in Appendices D–F. A comparison with experimental cross section data is made in Sec. VI, where we also discuss implications and future directions.

II. BETHE-SALPETER BASICS

Recall the definition of the nucleon-nucleon potential from the Bethe-Salpeter formalism. We follow the approach of Partovi and Lomon [17] and also consider the relationship between the Bethe-Salpeter wave function and the usual equal time wave function as recently discussed in Ref. [18].

Partovi and Lomon write the Bethe-Salpeter equation for the nucleon-nucleon scattering amplitude $\mathcal{M}$ as

$$\mathcal{M} = K + KG\mathcal{M}, \tag{1}$$

where K is the sum of all irreducible diagrams. The quantities $\mathcal{M}$ and K depend on the total four-momentum $P_{\rm tot}$ and the relative four-momentum k. The two individual momenta are $p_{1,2} = P_{\rm tot}/2 \pm k$ and G is the product of two Feynman propagators:

$$G = \left(\frac{i}{\not{p}_1 - m_N + i\epsilon}\right)_1 \left(\frac{i}{\not{p}_2 - m_N + i\epsilon}\right)_2 = G_1 G_2, \tag{2}$$

where m_N is the nucleon mass. The quantities $\mathcal{M}$ and K differ from those of [17] by a factor of $-i/(2\pi)$. Partovi and Lomon replace the relativistic G by the Lippmann-Schwinger propagator g for two particles. For scalar particles, g is obtained from G by integrating over the zeroth (energy) component of one of the two particles [18]. For fermions, one must also project onto the positive energy subspace of both particles. This is accomplished in the center of mass frame by taking [17]

$$g(k|P_{\rm tot}) = 2\pi i \frac{[\gamma^0 E(\mathbf{k}) - \boldsymbol{\gamma}\cdot\mathbf{k} + m_N]_1 [\gamma^0 E(\mathbf{k}) + \boldsymbol{\gamma}\cdot\mathbf{k} + m_N]_2}{E(\mathbf{k})\left(P_{\rm tot}^2 - 4m_N^2 - 4\mathbf{k}^2 + i\epsilon\right)} \delta(k^0), \tag{3}$$

where $E(\mathbf{k}) \equiv \sqrt{\mathbf{k}^2 + m_N^2}$. Note that g contains the important two-nucleon unitary cut. The nonrelativistic potential U is defined so as to reproduce the correct on-shell NN scattering amplitude $\mathcal{M}$ using the Lippmann-Schwinger (LS) equation

$$\mathcal{M} = U + Ug\mathcal{M}. \tag{4}$$

The quantity U is obtained by equating the $\mathcal{M}$ of Eq. (1) with that of Eq. (4) to find [17]

$$U = K + K(G - g)U. \tag{5}$$

In solving Eq. (4) for the on-energy shell scattering amplitude, U never changes the value of the relative energy k^0 away from 0. Equations (4) and (5) are consistent with Weinberg power counting in which one calculates the potential using chiral perturbation theory and then solves the LS equation to all orders. The term $G - g$ may be thought of a purely relativistic effect arising from off-shell (short-lived) intermediate nucleons, and in the present context a perturbative effect.

Consider the deuteron wave function in the final state of a pion production reaction. For P^2 near the pole position, the

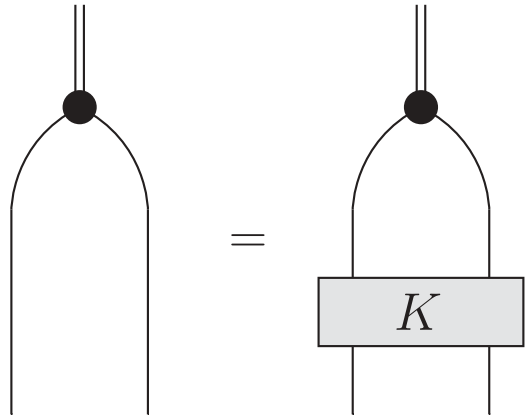

FIG. 2. Bethe-Salpeter equation near the deuteron pole.

second term of Eq. (1) dominates and we replace the scattering amplitude with the vertex function Γ: $\mathcal{M} \to \Gamma$, and

$$\Gamma = KG\Gamma. \tag{6}$$

This equation is shown pictorially in Fig. 2. The Bethe-Salpeter wave function Ψ is defined as $G\Gamma$ so that

$$\Psi = G\Gamma = GK\Psi. \tag{7}$$

The wave functions of the scattering state and the deuteron are shown in Fig. 3. If one uses Eq. (4), the bound-state wave function ϕ is obtained by solving the equation

$$\phi = gU\phi = gUgU\phi. \tag{8}$$

The second equation shows that U also is evaluated at vanishing values of time components of the relative momenta. We will treat the amplitudes Ψ, ϕ and the state vectors $|\Psi\rangle$, $|\phi\rangle$ (either bras or kets) as interchangeable.

The next step is to relate Ψ with ϕ, which can be thought of as the usual bound-state wave function. This is most easily accomplished by using the projection operator P on the product space of two positive-energy on-mass-shell nucleons. We then have

$$PG = GP \equiv G_P = g, \tag{9}$$

with the last step resulting from the explicit appearance of two positive-energy projection operators for on-mass-shell nucleons in Eq. (3). We define $Q = I - P$ and use the notation $\Psi_P \equiv P\Psi$, $\Psi_Q \equiv Q\Psi$ and $PKP \equiv K_{PP}$, $PKQ \equiv K_{PQ}$, etc. The Q space includes all terms with one or both nucleons off the mass shell. The amplitude Ψ_P contains the ordinary nucleonic degrees of freedom so one expects that it corresponds to ϕ. This is now shown explicitly. Use $I = P + Q$ in Eq. (7) and multiply by P and then also by Q to obtain the coupled-channel version of the relativistic bound state equation:

$$\Psi_P = G_P K_{PP}\Psi_P + G_P K_{PQ}\Psi_Q, \tag{10}$$

$$\Psi_Q = G_Q K_{QP}\Psi_P + G_Q K_{QQ}\Psi_Q. \tag{11}$$

Solving Eq. (11) for Ψ_Q and using the result in Eq. (10) gives

$$\Psi_Q = [1 - G_Q K_{QQ}]^{-1} G_Q K_{QP}\Psi_P, \tag{12}$$

$$\Psi_P = G_P \left(K_{PP} + K_{PQ}\left[G_Q^{-1} - K_{QQ}]big\right]^{-1} K_{QP}\right)\Psi_P, \tag{13}$$

but one can multiply Eq. (5) by $P \cdots P$, etc. to obtain the result

$$U_{PP} = K_{PP} + K_{PQ}\left[G_Q^{-1} - K_{QQ}\right]^{-1} K_{QP}, \tag{14}$$

thus Eq. (13) can be re-expressed as

$$\Psi_P = G_P U_{PP}\Psi_P = gU\Psi_P. \tag{15}$$

This last equation is identical to Eq. (7). Thus we have the result that

$$\Psi_P = \phi. \tag{16}$$

Ψ_P is not the complete wave function, but we expect that Ψ_Q is a perturbative correction because the deuteron is basically a nonrelativistic system.

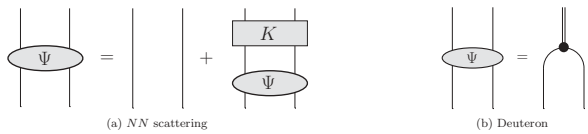

FIG. 3. Bethe-Salpeter wave functions.

III. THE $N \to N\pi$ AMPLITUDE

We now turn to the application of the Bethe-Salpeter formalism to the problem of threshold pion production. First, we remind the reader of the one-body pion production operator in baryon chiral perturbation theory (BChPT) [19]. For a modern review, see Ref. [20]. In this theory, the nucleon field is split into its heavy (H_v) and light (N_v) components,

$$\begin{aligned} \Psi(x) &= e^{-im_N v\cdot x}\left[N_v(x) + H_v(x)\right], \\ N_v(x) &= e^{im_N v\cdot x} P_+\Psi(x), \\ H_v(x) &= e^{im_N v\cdot x} P_-\Psi(x), \end{aligned} \tag{17}$$

where $P_\pm = (1 \pm \not{v})/2$ and v is the velocity vector satisfying $v^2 = 1$ and chosen in this work to be $v = (1, \mathbf{0})$. The heavy component is integrated out of the path integral and the resulting free equation of motion for the light component has a solution,

$$N(x) = \sqrt{E + m_N}\begin{pmatrix}\chi \\ 0\end{pmatrix} e^{-i(E-m_N)t + i\mathbf{p}\cdot\mathbf{x}}, \tag{18}$$

where $E = \sqrt{\mathbf{p}^2 + m_N^2}$ and χ is a two-component Pauli spinor. In Appendix B we show that the leading order (LO) Feynman rule for the s-wave $N \to N\pi$ amplitude vanishes at threshold and that the next-to-leading order (NLO) rule is

$$\mathcal{O}_\pi = -i\frac{m_\pi}{2m_N}\frac{g_A}{2f_\pi}\gamma^5\gamma_i\gamma^0(\overrightarrow{\nabla} - \overleftarrow{\nabla})_i\tau_a, \tag{19}$$

where the derivatives act on the nucleon wave functions.

IV. THE $NN \to d\pi$ REACTION: PLANE WAVE INITIAL STATES

Traditionally the impulse approximation to pion production is calculated by using the operator of Eq. (19) as the irreducible

kernel to be evaluated between nonrelativistic nucleon-nucleon wave functions for the initial and final states. Between two-component nucleon spinors $\gamma^5\gamma_i\gamma^0 \to \sigma_i$, so

$$\mathcal{M}_{1B}^{PW} = \langle\phi|\left[-i\frac{m_\pi}{2m_N}\frac{g_A}{2f_\pi}\boldsymbol{\sigma}\cdot(\overrightarrow{\nabla}-\overleftarrow{\nabla})\tau_a\right]|p_1, p_2\rangle, \quad (20)$$

where the superscript on $\mathcal{M}$ indicates that we have neglected initial state interactions. Next, we show that Eq. (20) is only an approximation to the full impulse amplitude derived from the relativistic Bethe-Salpeter formalism. We will see that this approximation is only valid in the absence of initial state interactions.

For the case of plane waves in both the initial and final states, a one-body operator is forbidden by energy-momentum conservation,

$$\langle p_3, p_4|\mathcal{O}_\pi|p_1, p_2\rangle = 0, \quad (21)$$

with all the p_i on mass shell. The correct formalism must be able to explain the required energy transfer. Our primary thesis is that the diagram of Fig. 1 must be obtained from the Feynman rules as

$$\mathcal{M}_{2B}^{PW} = \langle\Gamma|G_1\mathcal{O}_\pi|p_1, p_2\rangle = \langle\Psi|K(m_\pi/2)\,G_1\mathcal{O}_\pi|p_1, p_2\rangle, \quad (22)$$

where G_1 is the Feynman propagator of the intermediate off-shell nucleon and $K(m_\pi/2)$ is the sum of all irreducible diagrams with energy transfer of $m_\pi/2$. The second equality of Eq. (22) results from the relation between Γ and Ψ in Eq. (7). This manipulation is necessary because $\langle\phi|$ will be used for evaluation instead of $\langle\Psi|$, meaning that the relative energy must remain zero in the final state. Thus the full kernel for pion production via the impulse approximation is $KG_1\mathcal{O}_\pi$ rather than just $\mathcal{O}_\pi$. Because $KG_1\mathcal{O}_\pi$ is a two-body operator, the momentum mismatch which suppresses the IA in the traditional treatment is removed.

There are two points to emphasize here. First, this treatment is not equivalent to the heavy meson exchange operators of Refs. [21,22] which are intended to account for the relativistic initial and final state interactions not present in phenomenological potentials. Second, although the assertion of Eq. (22) greatly changes the way impulse pion production is calculated, one should not perform the same manipulations for the similar impulse approximation to photodisintegration. The reason for this is simply that near threshold the nucleon remains essentially on-shell and the diagram is therefore clearly reducible.

Next, we use $\Psi = \Psi_P + \Psi_Q = \phi + \Psi_Q$ and focus on the ϕ term; the other term contains nonnucleonic physics and may be treated as a correction. Thus the impulse approximation is given by

$$\mathcal{M}_{2B}^{PW} \approx \langle\phi|K(m_\pi/2)\,G_1\mathcal{O}_\pi|p_1p_2\rangle. \quad (23)$$

Consider the space time structure of the product $G_1\mathcal{O}_\pi$. The relativistic propagator G_1 is decomposed into three terms: 1, γ^0, and γ^i. Between two-component nucleon spinors

$$\begin{aligned}\gamma^5\gamma_i\gamma^0 &\to \sigma_i,\\ \gamma^0\gamma^5\gamma_i\gamma^0 &\to \sigma_i,\\ \gamma^i\gamma^5\gamma_j\gamma^0 &\to 0,\end{aligned} \quad (24)$$

and so we can make the replacement

$$\begin{aligned}G_1\mathcal{O}_\pi &= i\frac{\not{p}_1 - \not{q} + m_N}{(p_1-q)^2 - m_N^2 + i\epsilon}\mathcal{O}_\pi\\ &\to i\frac{E(\mathbf{p}_1) - m_\pi + m_N}{-2E(\mathbf{p}_1)m_\pi + m_\pi^2 + i\epsilon}\mathcal{O}_\pi\\ &= \frac{i}{-m_\pi}\left(1 - \frac{m_\pi}{4m_N}\right)\mathcal{O}_\pi,\end{aligned} \quad (25)$$

where in the second line we have used that $E(\mathbf{p}_1) = m_N + m_\pi/2$ at threshold. Note that this propagator agrees with that obtained from the Feynman rules for BChPT at LO.

In order to make connection with the traditional Eq. (19), we use the approximations $K \approx U$ [corrections are $\mathcal{O}(g-G)$] and $G_1 \approx -i/m_\pi$ [corrections are $\mathcal{O}(m_\pi/m_N)$]. Putting these substitutions into Eq. (23),

$$\mathcal{M}_{2B}^{PW} \approx \langle\phi|\left[-\frac{iU\left(\frac{m_\pi}{2}\right)}{m_\pi}\mathcal{O}_\pi\right]|p_1p_2\rangle. \quad (26)$$

The quantity U is related to the potential energy by $U = -iV$. Ignoring the fact that U should be evaluated for nonzero energy transfer, we use the equal-time Schrödinger equation to replace $V \to -E_d - p^2/m_N$ and then neglect the binding energy to find $\mathcal{M}_{2B}^{PW} \approx \mathcal{M}_{1B}^{PW}$. This means that for a PW initial state, the traditional impulse approximation should be roughly adequate. This is borne out in the actual calculation of the reduced matrix

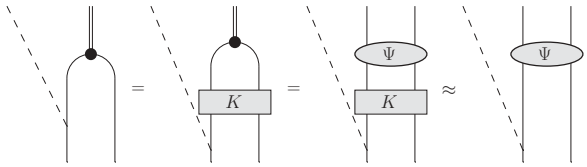

FIG. 4. Bethe-Salpeter formalism applied to pion production for plane wave initial states.

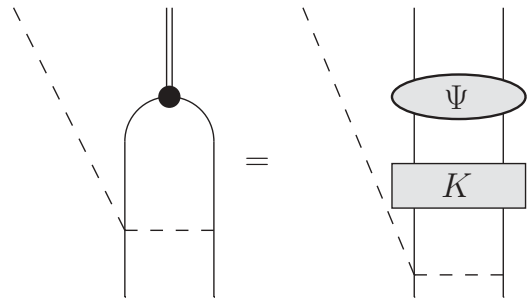

FIG. 5. Use of the Bethe-Salpeter equation in the rescattering amplitude.

elements for Eqs. (20) and (26),

$$A_{1B}^{PW} = -24.0, \tag{27}$$

$$A_{2B}^{PW} = -25.6, \tag{28}$$

where we have used Ref. [8]'s definition of the reduced matrix element (we suppress the subscript on Ref. [8]'s A_0 for clarity) and used the same static phenomenological potential for V (here, Argonne v18 [23]) that is used to calculate the wave functions. See Fig. 4 for a pictorial description of this section.

It is important to note that the Bethe-Salpeter equation can also be used for the pion rescattering diagram as shown in Fig. 5. In fact, the diagram on the right in Fig. 5 has played an important role in the development of pion production. The authors of Ref. [24] showed that this diagram (with K approximated by OPE) becomes irreducible when the energy dependence of the $NN\pi\pi$ vertex is used to cancel one of the intermediate nucleon propagators. This discovery resolved a problem arising from calculation of NLO loops.

In the next section we will show that for distorted wave initial states Eq. (26) is replaced by

$$\mathcal{M}_{2B}^{DW} \approx {}_f\langle\phi| \left[-\frac{iU\left(\frac{m_\pi}{2}\right)}{m_\pi}\mathcal{O}_\pi + \mathcal{O}_\pi \frac{iU\left(\frac{m_\pi}{2}\right)}{m_\pi} \right] |\phi\rangle_i, \tag{29}$$

where the first term contributes at leading order in the theory and the second term at next-to-leading order.

V. THE $NN \to d\pi$ REACTION: DISTORTED WAVE INITIAL STATES

A. Definition of distorted wave operator

There is no reason to expect the result $\mathcal{M}_{2B}^{PW} \approx \mathcal{M}_{1B}^{PW}$ to carry over for a distorted wave (DW) initial state where $\mathbf{p}^2 = m_\pi m_N$ no longer holds. Indeed, we will show that the traditional expression for the impulse approximation does not hold for DW amplitudes.

The fully relativistic initial-state wave function is denoted $|\Psi\rangle_i$

$$|\Psi\rangle_i = |p_1, p_2\rangle + GK|\Psi\rangle_i, \tag{30}$$

where the first term is exactly the initial state used in the definition of $\mathcal{M}^{PW}$ of Eqs. (20) and (22). The complete DW impulse operator is defined as

$$\mathcal{M}^{DW} = \mathcal{M}^{PW} + \mathcal{M}^{ISI}. \tag{31}$$

The second term includes the production operator $KG_1\mathcal{O}_\pi$ from Eq. (22) along with initial state interactions,

$$\mathcal{M}_{2B}^{ISI} = {}_f\langle\Psi|KG_1\mathcal{O}_\pi GK|\Psi\rangle_i \tag{32}$$

$$\approx {}_f\langle\phi|KG_1\mathcal{O}_\pi GK|\phi\rangle_i, \tag{33}$$

where in the second line we have once again used $\Psi = \phi + \Psi_Q$ and neglected the Q space.

As noted by Ref. [25], the kernel of Eq. (33) is a loop integral which is shown in Fig. 6 with K being approximated by OPE. Note that four momenta are conserved at every vertex. One pion exchange is the first contribution to K in ChPT besides a short range operator which is irrelevant for the s-wave $NN \to d\pi$ amplitude (see Appendix A). Nevertheless, one must exercise caution due to the large expansion parameter of pion production. To this end, we employ the deuteron of Ref. [26] which is calculated from a purely OPE potential with suitable form factors. As discussed in Appendix C, this deuteron wave function is quite accurate and increases the rescattering amplitude by only 3% over a phenomenological deuteron. Having then employed this deuteron wave function in the calculation of the traditional DW impulse approximation, we will be able to avoid any complications from higher order parts of the potential in our subsequent investigation of the two-body operator of Eq. (33). In other words, although the full potential must be present in an exact calculation, we expect to gain insight into the correct formalism by using an OPE-only deuteron. We continue to use the phenomenological potentials for the initial state. To verify that the use of $K =$ OPE in the initial state does not spoil our results too much, Appendix F examines heavy meson exchange in the initial state. As will be discussed, this effect is parametrically suppressed.

Note that the relative momenta of the nucleons before and after the loop ($\mathbf{p}$ and $\mathbf{k}$) are external momenta to the loop integral over $l = (l^0, \mathbf{l})$, but are eventually integrated over in a momentum-space evaluation. Let us focus solely on the energy part of the loop integral and ignore the vertex factors and overall constants. We define the integral I,

$$I = i^5 \int \frac{dl^0}{2\pi} \frac{1}{l^0 - E + i\epsilon} \frac{1}{l^0 - m_\pi - E + i\epsilon} \frac{1}{-l^0 + m_\pi - \gamma - E + i\epsilon} \frac{1}{l^0 - m_\pi/2 - \gamma/2 + \omega_i - i\epsilon} \times \frac{1}{l^0 - m_\pi/2 - \gamma/2 - \omega_i + i\epsilon} \frac{1}{l^0 - m_\pi + \gamma/2 + \omega_f - i\epsilon} \frac{1}{l^0 - m_\pi + \gamma/2 - \omega_f + i\epsilon}, \tag{34}$$

where $\omega_i^2 = (\mathbf{l} - \mathbf{p})^2 + m_\pi^2$ is the on-shell energy of the initial-state pion, $\omega_f^2 = (\mathbf{l} - \mathbf{k})^2 + m_\pi^2$ is the on-shell energy of the final state pion, and $E = \mathbf{l}^2/2m_N$ is the kinetic energy of a single intermediate nucleon. Note that $\mathbf{p}_i^2 \approx m_\pi m_N - \gamma m_N$ and $\mathbf{k}_f^2 \approx -\gamma m_N$.

It is straightforward to show that if the energy components of the exchanged pions in the above loop are set to zero (violating conservation of four momentum), one obtains the traditional impulse approximation. In this case, the pion energy denominators are pulled out of the integral which is then

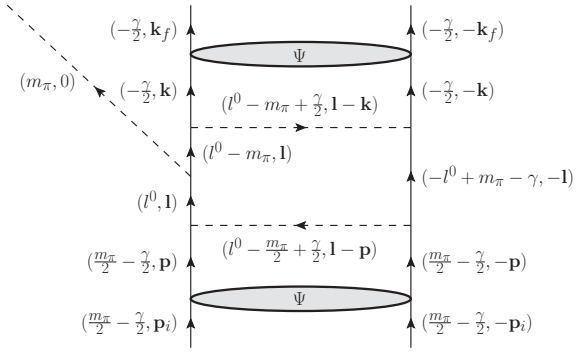

FIG. 6. Impulse approximation using distorted waves. Solid lines represent nucleons, dashed lines represent pions, and ovals represent wave functions.

evaluated by closing the contour in the lower half plane,

$$I_{1\mathrm{B}}=\left(\frac{1}{-\omega_f^2}\,\frac{1}{-\gamma-\mathbf{l}^2/m_N}\right)\left(\frac{1}{m_\pi-\gamma-\mathbf{l}^2/m_N}\,\frac{1}{-\omega_i^2}\right). \tag{35}$$

The quantity in the first set of parentheses can be recognized as the product of OPE with the final state wave function while the second set is the product of the initial state wave function with OPE. This is precisely the operator that the traditional evaluation includes.

B. Reduction to time ordered perturbation theory (TOPT)

Our goal is to evaluate the integral in Eq. (34), showing that it is a sum of TOPT terms which can be combined to obtain Eq. (29). To begin, we rewrite the first two factors as a sum,

$$\frac{1}{l^0-E+i\epsilon}\,\frac{1}{l^0-m_\pi-E+i\epsilon}=\frac{1}{-m_\pi}\left(\frac{1}{l^0-E+i\epsilon}-\frac{1}{l^0-m_\pi-E+i\epsilon}\right). \tag{36}$$

This is the key to our method because after making this split we see two terms which each have the propagator structure of a rescattering box loop. Consider the first term in Eq. (36); this loop integral looks like a two-body operator multiplied by $\frac{1}{-m_\pi}$ and augmented with an initial-state interaction. The second term looks like the same with final-state interaction. We define these two integrals to be $I^a_{2\mathrm{B}}$ and $I^b_{2\mathrm{B}}$, respectively,

$$I_{2\mathrm{B}}=I^a_{2\mathrm{B}}+I^b_{2\mathrm{B}}. \tag{37}$$

Figure 7 illustrates the splitting described in Eq. (37).

Next, we perform partial fraction decomposition on each of the pion propagators, splitting each of the two terms into four terms. Then we continue the decomposition process until each term can be expressed as a single residue. For $I^a_{2\mathrm{B}}$ we will isolate the poles containing ω_f and then close the contour around them (for $I^b_{2\mathrm{B}}$, the ω_i poles are isolated). By isolating the poles in this way, the resulting expression is easily recognized as the sum of six TOPT terms. For clarity, we show these terms pictorially for $I^a_{2\mathrm{B}}$ in Fig. 8 where we have left the overall $\frac{1}{-m_\pi}$ implicit.

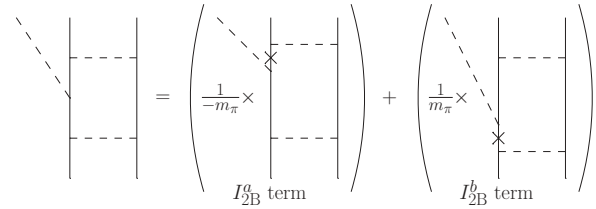

FIG. 7. Definition of the two terms in Eq. (37). Crosses represent the propagators which are absent due to the partial fractions decomposition.

We assume for now that the stretched box diagrams are small, as they were in the rescattering toy model investigation [27] and denote the sum of the four remaining terms with a $\mathring{I}$.

Finally, motivated by the interpretation which is presented in the next section, we algebraically re-combine these four terms to find

$$\mathring{I}^a_{2\mathrm{B}}=\frac{1}{(m_\pi/2)^2-[\omega_f+\delta_a(\mathbf{l})]^2}\left[1+\frac{\delta_a(\mathbf{l})}{\omega_f}\right]\frac{1}{-m_\pi}\times\left[1-\frac{\delta_a(\mathbf{l})}{\omega_i+\delta_a(\mathbf{l})}\right]\frac{1}{m_\pi-2E-\gamma}\,\frac{1}{-\omega_i^2}, \tag{38}$$

$$\mathring{I}^b_{2\mathrm{B}}=\frac{1}{-\omega_f^2}\,\frac{1}{-2E-\gamma}\left[1-\frac{\delta_b(\mathbf{l})}{\omega_f+\delta_b(\mathbf{l})}\right]\frac{1}{m_\pi}\times\left[1+\frac{\delta_b(\mathbf{l})}{\omega_i}\right]\frac{1}{(m_\pi/2)^2-[\omega_i+\delta_b(\mathbf{l})]^2}, \tag{39}$$

where we have separated out terms involving δ_a and δ_b,

$$\delta_a(\mathbf{l})=\frac{\mathbf{l}^2}{2m_N}-\frac{m_\pi}{2}+\frac{\gamma}{2}, \tag{40}$$

$$\delta_b(\mathbf{l})=\frac{\mathbf{l}^2}{2m_N}+\frac{\gamma}{2}, \tag{41}$$

because (as will be shown in the next section) they are subleading and we will neglect them in the main body of this work. The only approximation made in the evaluation of the loop integral to obtain Eqs. (38) and (39) is to neglect the stretched boxes. Let us pause to summarize what we have done so far: (1) the DW amplitude was written down as a loop integral, (2) partial fractions was used to split the product of the two nucleon propagators into a sum $I^a_{2\mathrm{B}}+I^b_{2\mathrm{B}}$, (3) the loop integrals were evaluated and the result expressed in terms of TOPT diagrams, and (4) the TOPT diagrams were algebraically combined into a form useful for the following interpretation.

C. Interpretation

Although not obvious at first sight, convolution of the operator corresponding to Eq. (38) with wave functions as defined in Eqs. (31) and (33) results in an amplitude approximately equivalent to that which one obtains by using the operator shown in Fig. 9(a). The same is true of Eq. (39) with Fig. 9(b), and together they replace the traditional (one-body) impulse approximation with Eq. (29). Furthermore, the operator that results from Eq. (39) is expected to be small by

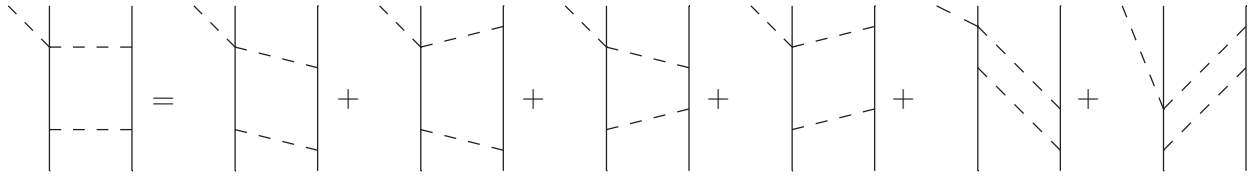

FIG. 8. TOPT terms resulting from the $I^a_{2\mathrm{B}}$ integral.

power counting arguments. The task of this subsection is to verify these statements in detail.

In Eq. (38) the factor $(m_\pi - 2E - \gamma)^{-1}(-\omega_i^2)^{-1}$ is interpreted as the product of the two-nucleon initial-state wave function with static OPE. This is the statement that

$$\frac{1}{m_\pi - 2E - \gamma}\frac{1}{-\omega_i^2} = gU^{\mathrm{OPE}}. \tag{42}$$

This factor can be absorbed (after adding in the PW term) using the zero-relative-energy Lippmann-Schwinger equation that is employed by the phenomenological potentials we are using. We will continue to refer to the initial wave function as a function of $\mathbf{p}$ and $\mathbf{p}_i$, so absorbing this factor means that we set $\mathbf{l} = \mathbf{p}$.

Likewise, in Eq. (39) the factor $(-\omega_f^2)^{-1}(-2E - \gamma)^{-1}$ is interpreted as the product of static OPE with the two-nucleon final-state wave function: $U^{\mathrm{OPE}}g$. Absorbing this factor into the wave function, we set $\mathbf{l} = \mathbf{k}$. The remaining factors of $\mathring{I}^a_{2\mathrm{B}}$ and $\mathring{I}^b_{2\mathrm{B}}$ become the two-body impulse production operators,

$$\mathcal{O}^a_{2\mathrm{B}} = \frac{\boldsymbol{\sigma}_1\cdot(\mathbf{p}-\mathbf{k})\boldsymbol{\sigma}_2\cdot(\mathbf{k}-\mathbf{p})}{(m_\pi/2)^2 - [\omega_f + \delta_a(\mathbf{p})]^2}\left[1 + \frac{\delta_a(\mathbf{p})}{\omega_f}\right]\frac{1}{-m_\pi} \times \left[1 - \frac{\delta_a(\mathbf{p})}{\omega_i + \delta_a(\mathbf{p})}\right]\mathbf{S}\cdot\mathbf{p}, \tag{43}$$

$$\mathcal{O}^b_{2\mathrm{B}} = \mathbf{S}\cdot\mathbf{k}\left[1 - \frac{\delta_b(\mathbf{k})}{\omega_f + \delta_b(\mathbf{k})}\right]\frac{1}{m_\pi} \times \left[1 + \frac{\delta_b(\mathbf{k})}{\omega_i}\right]\frac{\boldsymbol{\sigma}_1\cdot(\mathbf{p}-\mathbf{k})\boldsymbol{\sigma}_2\cdot(\mathbf{k}-\mathbf{p})}{(m_\pi/2)^2 - [\omega_i + \delta_b(\mathbf{k})]^2}, \tag{44}$$

where we have now made explicit the momentum dependences of the vertices and used $\mathbf{S} = (\boldsymbol{\sigma}_1 + \boldsymbol{\sigma}_2)/2$. It is also important to include form factors in the OPE which match those of the wave functions. These form factors are present in our calculation even though we leave them out of this expression for the sake of generality.

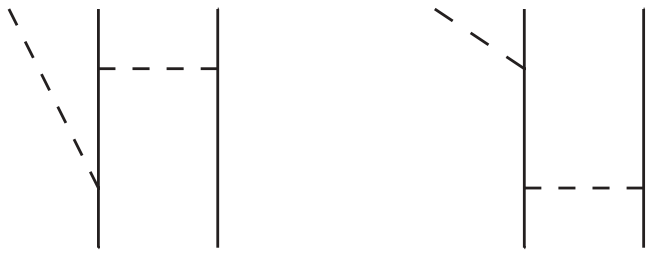

(a) $\mathcal{O}^a_{2\mathrm{B}}$ of Eq. (45) (b) $\mathcal{O}^b_{2\mathrm{B}}$ of Eq. (46)

FIG. 9. Two-body impulse production operators (pion exchange is nonstatic).

Next, note that in the evaluation of the matrix element using Eq. (43), the initial state wave function is peaked about its plane wave value $\mathbf{p} \approx \mathbf{p}_i$, and thus $E \approx m_\pi/2 - \gamma/2$ and $\delta_a(\mathbf{p}) \approx 0$. On the other hand, in Eq. (44), we have $\mathbf{k} \approx \mathbf{k}_i$ and $E \approx -\gamma/2$ and $\delta_b(\mathbf{k}) \approx 0$. If we were to neglect all the δ, we would have

$$\mathcal{O}^a_{2\mathrm{B}} \approx \frac{\boldsymbol{\sigma}_1\cdot(\mathbf{p}-\mathbf{k})\boldsymbol{\sigma}_2\cdot(\mathbf{k}-\mathbf{p})}{(m_\pi/2)^2 - \left[(\mathbf{p}-\mathbf{k})^2 + m_\pi^2\right]}\frac{1}{-m_\pi}\mathbf{S}\cdot\mathbf{p}, \tag{45}$$

$$\mathcal{O}^b_{2\mathrm{B}} \approx \mathbf{S}\cdot\mathbf{k}\frac{1}{m_\pi}\frac{\boldsymbol{\sigma}_1\cdot(\mathbf{p}-\mathbf{k})\boldsymbol{\sigma}_2\cdot(\mathbf{k}-\mathbf{p})}{(m_\pi/2)^2 - \left[(\mathbf{p}-\mathbf{k})^2 + m_\pi^2\right]}, \tag{46}$$

which suggests that these operators can be approximately interpreted as the diagrams in Fig. 9. Thus we have finally obtained our central result [Eq. (29)] which states that the correct impulse approximation is a two-body operator. The contribution to pion production given in Eq. (29) is not replacing the rescattering diagram (which is also two body), but rather replacing the traditional contribution which has been referred to as the impulse approximation (or direct production). Note that if we assign standard pion production power counting to these diagrams, Fig. 9(a) is $\mathcal{O}(\sqrt{\frac{m_\pi}{m_N}})$ while Fig. 9(b) is $\mathcal{O}(\frac{m_\pi}{m_N})$. In the next section the approximate expressions given in Eqs. (45) and (46) are numerically evaluated. Nevertheless, we acknowledge the importance of verifying that the δ terms are indeed small and relegate that discussion to Appendices D and E.

D. Evaluation of two-body operators

Next, we calculate the threshold s-wave $np \to d\pi^0$ amplitudes corresponding to Eqs. (45) and (46). We do not present the details here as most are given in Ref. [13]. Again, we remind the reader that for the sake of consistency we use a deuteron wave function calculated from a purely OPE potential (with form factors as described in Appendix C). For the initial-state distorted waves, we use three different phenomenological potentials (Av18 [23], Nijmegen II [28], and Reid '93 [28]). In Table I we display the results in terms of the reduced matrix elements of Ref. [8].

The first row of Table I gives the traditional (one-body) impulse approximation, which is slightly bigger than Ref. [13] due to the use of the OPE deuteron. The next row shows that the new two-body operator (at leading order) is roughly twice as large as the traditional calculation it is replacing. We mention here that the significant cancellation between deuteron s and d states remains, keeping the impulse amplitude smaller than rescattering; however, the cancellation is less complete when using our new two-body operator. The final row verifies that the $\mathcal{O}^b_{2\mathrm{B}}$ diagram is smaller than the $\mathcal{O}^a_{2\mathrm{B}}$ diagram, as dictated

TABLE I. Threshold reduced matrix elements calculated with an OPE deuteron and various phenomenological initial states. The first row shows the traditional impulse approximation (one-body) while the second and third show our replacement (two-body).

	Av18	Reid'93	Nijm II
A_{1B}^{DW}	8.3	7.1	5.4
$A_{2B}^{DW,a}$	17.4	13.5	7.8
$A_{2B}^{DW,b}$	−1.5	−2.2	−6.9

by the power counting. The Nijmegen II potential provides a bit of deviation from these results, and it will be interesting to investigate other potentials to determine the true model dependence of this calculation. In finding these results, it is important that the pion propagators of Eqs. (45) and (46) be implemented in a manner consistent with the potential used for the wave function of Fig. 6. Namely the cutoff procedure of the convolution integral with form factors needs to match that by which the potential was constructed. Appendix C contains the details of this procedure.

Our conclusion is that the traditional impulse approximation is an underestimate. While it is true that several approximations were made in order to permit final expressions as simple as Eqs. (45) and (46), we believe this conclusion to be sound. The δ terms do not defy their classification as subleading (see Appendices D and E), and Appendix F shows that using $K =$ OPE in the initial state is at least reasonable. In summary, we simply claim that Eq. (45) is the new impulse approximation at leading order in the effective field theory. The corrections in the aforementioned appendices, in addition to Eq. (46) contribute to the next-to-leading order calculation, which needs to be systematically considered in a later work.

Finally, it is important to note that although the OPE deuteron reproduces the phenomenological results for the rescattering diagram quite well, the numbers in this section are greatly changed if a phenomenological deuteron is used. Using Av18 we find $A_{1B}^{DW} = 4.9$, and by using the cutoff procedure of Av18 for the two-body operators, we find $A_{2B}^{DW,a} = 33.5$, $A_{2B}^{DW,b} = -2.8$. Thus the ratio of our new two-body operator to the traditional impulse operator is ∼7 instead of the ∼2 presented above. At this time one is faced with a choice of either: (1) using a "correct" phenomenological deuteron and leaving out parts of the potential when calculating the two-body kernel or (2) using an inexact OPE deuteron with a completely self-consistent kernel. For the time being we believe the latter to be more trustworthy, if not ideal.

VI. DISCUSSION

Experimental data for pion production near threshold are reported in terms of two parameters, α and β, defined for $np \to d\pi^0$,

$$\sigma(\eta) = \tfrac{1}{2}\left(\alpha\eta + \beta\eta^3\right), \tag{47}$$

where η is the pion momentum in units of its mass. Table VI of Ref. [13] shows the results obtained by the four most recent

TABLE II. Threshold reduced matrix elements extracted from experiment.

Experiment	A^{expt}
$np \to d\pi^0$ [29]	80.1 ± 1.1
$\vec{p}p \to d\pi^+$ (Coulomb corrected) [30]	85.2 ± 1.0
$pp \to d\pi^+$ (Coulomb corrected) [31]	84.6 ± 1.9
Pionic deuterium decay [32]	$93.8^{+0.9}_{-2.0}$

experiments. Since the present calculation is performed at threshold ($\eta = 0$), we compute only the value of α,

$$\alpha = \frac{m_\pi}{128\pi^2 sp}\,|A|^2\,, \tag{48}$$

where $s = (m_d + m_\pi)^2$ is the square of the invariant energy. For ease of comparison, we invert Eq. (48), plug in the results of the mentioned experiments, and propagate the errors to find Table II.

The full theoretical amplitude includes not only the impulse diagram but also the rescattering diagram, which is given in Table III along with the total amplitude using either the traditional one-body or the leading-order two-body impulse diagram. The uncertainty in an effective field theory calculation is estimated by the power counting scheme. In this work, we have included both the rescattering and the impulse diagrams up to $\mathcal{O}(\sqrt{m_\pi/m_N})$. Therefore one might assign an uncertainty of $m_\pi/m_N = 14\%$ to the calculation but stress that such an estimate based solely on power counting is rough at best. Taking this uncertainty, we see that the theory update presented here changes the situation from underprediction of the most recent pionic deuterium experiment by $\sim 1.3\,\sigma$, to underprediction by $\sim 0.7\,\sigma$.

In summary, we have developed a consistent formalism that allows one to separate effects of the kernel from those of the wave functions, finding a new impulse approximation kernel. This two-body operator, given in Eq. (29), replaces the traditional one-body impulse approximation and is the central result of the present work. We numerically investigated the simplest example (s-wave $NN \to d\pi$) and found the impulse amplitude to be increased by a factor of roughly 2 over the traditional amplitude. This calculation was performed with a regulated OPE deuteron which has advantages and disadvantages as described in the body of this work. Rescattering remains the dominant contribution to the cross section. We find that the updated total cross section is ∼10% larger than before and is in agreement with experiment at leading order. We verified that corrections to the new

TABLE III. Rescattering (RS) and total reduced matrix elements for a variety of potentials. The second line shows the traditional calculation (with a one-body IA) while the third shows our replacement (with a two-body IA).

	Av18	Reid '93	Nijm II
RS	69.8	72.1	74.0
RS + IA (1B)	78.1	79.2	79.4
RS + IA (2B)	87.2	85.6	81.8

impulse approximation (which together with other loops and counterterms will contribute at next-to-leading order) do not destroy these results.

These findings suggest several directions for future research. First, one needs to develop a power counting scheme for the "Q space" discussed in Sec. II. Second, the significant model dependence of the new formulation of the impulse approximation needs to be investigated in a renormalization group invariant way. Third, it will be very interesting to see the impact of this increased impulse amplitude on the $pp \to pp\pi^0$ cross section which is suppressed due to the absence of rescattering. Finally, one could look at the energy dependence (p-wave pions) of $NN \to NN\pi$, for which there is an abundance of experimental data.

ACKNOWLEDGMENTS

This research was supported in part by the US Department of Energy. We thank Christoph Hanhart and Vadim Baru for multiple valuable conversations and for suggesting the investigation of the full loop integral.

APPENDIX A: LAGRANGE DENSITIES

We define the index of a Lagrange density to be

$$\nu = d + \frac{f}{2} - 2, \tag{A1}$$

where d is the sum of the number of derivatives and powers of m_π, and f is the number of fermion fields. This represents the standard power counting for nuclear physics. The $\nu = 0$ Lagrangian (with spatial vectors in bold font) is [10]

$$\mathcal{L}^{(0)} = \tfrac{1}{2}(\partial\pi_a)^2 - \tfrac{1}{2}m_\pi^2\pi_a^2 + N^\dagger i\partial_0 N + \frac{g_A}{2f_\pi}N^\dagger(\tau_a\boldsymbol{\sigma}\cdot\boldsymbol{\nabla}\pi_a)N + \cdots, \tag{A2}$$

where τ_a and $\boldsymbol{\sigma}$ are the Pauli matrices acting on the isospin and spin of a single nucleon. The "$+\cdots$" indicates that only the terms used in this calculation are shown.

The $\nu = 1$ Lagrangian includes recoil corrections and other terms invariant under $\mathrm{SU}(2)_L \times \mathrm{SU}(2)_R$,

$$\mathcal{L}^{(1)} = \frac{1}{2m_N}N^\dagger\boldsymbol{\nabla}^2 N - \frac{1}{2m_N} \times \left(\frac{g_A}{2f_\pi} i N^\dagger\tau_a\dot{\pi}_a\boldsymbol{\sigma}\cdot\boldsymbol{\nabla}N + \text{H.c.}\right) + \cdots, \tag{A3}$$

where we use the values given in Table IV. Note that the terms with the c_i low energy constants which appear at this order do not get promoted in MCS for these kinematics and are thus not used. Also, the terms with the d_i low energy constants do not contribute to s-wave pion production. Finally, the $NNNN$ contact terms $C_{S,T}$ do not contribute because we are using a potential with a repulsive core [$R_i(r)R_f(r) \to 0$ as $r \to 0$ for $l_i = 1, l_f = 0$].

TABLE IV. Parameters used.

$m_\pi = 134.98$ MeV	$g_A = 1.32$ MeV
$m_N = 938.92$ MeV	$f_\pi = 92.4$ MeV

APPENDIX B: $N \to N\pi$ FROM BCHPT

The LO $NN\pi$ interaction reads

$$\mathcal{L}^{(0)} \subset \overline{N}\frac{g_A}{2}\not{u}_\perp\gamma^5 N, \tag{B1}$$

where $u_{\perp,\mu} = u_\mu - v\cdot u\, v_\mu$, $u_\mu = i(u^\dagger\partial_\mu u - u\partial_\mu u^\dagger)$ and $u^2 = e^{i\tau_a\pi_a/f_\pi}$. We find

$$u_\mu = i\left[i\tau_a\partial_\mu\frac{\pi_a}{2f_\pi} - (-i)\tau_a\partial_\mu\frac{\pi_a}{2f_\pi}\right] = -\frac{\tau_a}{f_\pi}\partial_\mu\pi_a,$$

$$u_\perp = \gamma_0(u_0 - u_0\cdot 1) - \gamma_i\left(-\frac{\tau_a}{f_\pi}\partial_i\pi_a\right), \qquad i = 1,\ 2,\ 3,$$

$$= \frac{\tau_a}{f_\pi}\gamma_i\partial_i\pi_a, \tag{B2}$$

and thus the Feynman rule for an outgoing pion with momentum q and isospin a is

$$\mathcal{O}_\pi^{(0)} = -i\left(\frac{g_A}{2f_\pi}\gamma_i\gamma^5\right)(iq_i)\tau_a. \tag{B3}$$

At threshold, the pion four momentum is $q = (m_\pi, 0, 0, 0)$ making $\mathcal{O}_\pi^{(0)} = 0$. This reflects the fact (well-known from current algebra) that threshold pion production proceeds via the off-diagonal, and therefore $1/m_N$ suppressed, interaction $g_\pi\gamma^5\gamma^0 q^0\tau$. In the effective theory, this recoil correction shows up in the NLO Lagrangian

$$\mathcal{L}^{(1)} \subset -i\frac{g_A}{2m_N}\overline{N}\{v^\mu u_\mu, S^\mu\partial_\mu\}N, \tag{B4}$$

where the spin vector is $S^\mu = -\frac{1}{2}\gamma^5(\gamma^\mu\not{v} - v^\mu)$. Thus the Feynman rule is

$$\mathcal{O}_\pi^{(1)} = -i\left(-i\frac{g_A}{2m_N}\right)\left[-\frac{\tau_a}{f_\pi}(-im_\pi)\right] \times\left[\frac{1}{2}\gamma^5\gamma_i\gamma^0(\overrightarrow{\boldsymbol{\nabla}} - \overleftarrow{\boldsymbol{\nabla}})_i\right] = -i\frac{m_\pi}{2m_N}\frac{g_A}{2f_\pi}\gamma^5\gamma_i\gamma^0(\overrightarrow{\boldsymbol{\nabla}} - \overleftarrow{\boldsymbol{\nabla}})_i\tau_a, \tag{B5}$$

where the derivatives act on the nucleon wave functions.

APPENDIX C: ONE PION EXCHANGE DEUTERON

In this Appendix we present the method by which the deuteron wave function is calculated for use in Sec. V. This method is taken directly from the work of Friar, Gibson, and Payne [26]. The OPE potential is defined to have central (Y) and tensor (T) parts,

$$V_\pi(\mathbf{r}) = f^2 m_\pi\frac{\tau_{1,a}\tau_{2,a}}{3}[\boldsymbol{\sigma}_1\cdot\boldsymbol{\sigma}_2 Y(r) + S_{12}T(r)], \tag{C1}$$

where $f^2 = 0.079$ (to be distinguished from f_π) measures the strength of the pion-nucleon coupling and S_{12} is the standard

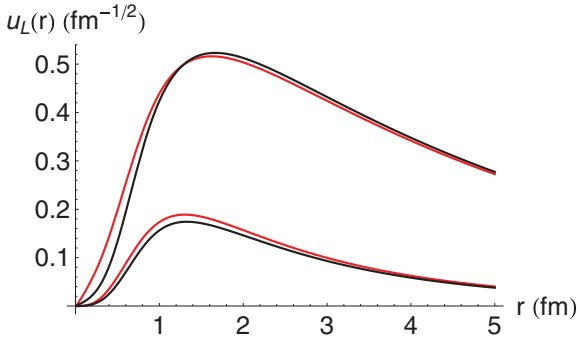

FIG. 10. (Color online) Deuteron s- and d-state wave functions (the s state is larger). The potentials used to calculate the wave functions are Av18 (black) and the cutoff OPE described in this section (red).

tensor operator. The deuteron has isospin zero and spin one, so we have

$$V_\pi(\mathbf{r}) = -f^2 m_\pi \left[Y(r) + S_{12}T(r)\right]. \tag{C2}$$

The Y and T functions are expressed as derivatives of the Fourier transform of the pion propagator,

$$\begin{aligned} Y(r) &= h_0''(x) - h_0'(x)/x, \\ T(r) &= h_0''(x) + 2h_0'(x)/x, \\ h_0(x) &= \frac{4\pi}{(2\pi)^3 m_\pi}\int d^3q \frac{e^{-i\mathbf{q}\cdot\mathbf{r}}}{\mathbf{q}^2+m_\pi^2} F_{\pi NN}^2(\mathbf{q}^2), \end{aligned} \tag{C3}$$

where $x = m_\pi r$ and $F_{\pi NN}$ is the form factor for which we use

$$F_{\pi NN}(\mathbf{q}^2) = \left(\frac{\Lambda^2 - m_\pi^2}{\mathbf{q}^2+\Lambda^2}\right)^n. \tag{C4}$$

In Ref. [26] it is shown that

$$Y(r) = \frac{e^{-x}}{x} - \beta^3 e^{-\beta x}\sum_{i=0}^{2n-1}\frac{\xi^i}{i!}[\delta_i(\beta x) - 2i\delta_{i-1}(\beta x)], \tag{C5}$$

$$\begin{aligned} T(r) = {} & \frac{e^{-x}}{x}\left(1+\frac{3}{x}+\frac{3}{x^2}\right) \\ & - \beta^3 e^{-\beta x}\sum_{i=0}^{2n-1}\frac{\xi^i}{i!}[\delta_i(\beta x) - (2i-3)\delta_{i-1}(\beta x)], \end{aligned} \tag{C6}$$

where $\beta = \Lambda/m_\pi$ and $\xi = (\beta^2-1)/2\beta^2$ and the δ_i are defined by

$$\delta_{i+1}(\beta x) = (2i-1)\delta_i(\beta x) + (\beta x)^2\delta_{i-1}(\beta x) \tag{C7}$$

along with $\delta_0 = 1/\beta x$ and $\delta_1 = 1$. One of the results of Ref. [26] is that larger values of n lead to better fits to experimental data. We use $n = 5$ and $\beta/\sqrt{10} = 5.687805$ in order to precisely reproduce the binding energy $E_B = 2.2246$ MeV. The wave functions are calculated by integrating in from $r_{\max} = 100$ fm and adding together two linearly independent solutions such that the sum vanishes at $r_{\min} = 0.01$ fm. As shown in Fig. 10, the results are close to the "correct" Av18 deuteron.

In Table V we display the quadrupole moment and mean square charge radius of Av18, this OPE potential, and experiment (as quoted in [26]). It is clear that the form factors in the OPE potential make it difficult to distinguish this construction as less accurate than Av18. Finally, in Table VI we display the reduced matrix elements for the rescattering pion production diagram evaluated with both the phenomenological potentials and the deuteron of this section. Since this diagram makes the largest contribution to the cross section we need to verify that neglecting non-OPE parts of the potential does not dramatically change this amplitude.

TABLE V. Deuteron properties.

Potential	Q (fm^2)	$\langle r^2\rangle^{1/2}$ (fm)
Av18	0.270	1.968
OPE ($n = 5$)	0.282	1.939
Experiment	0.2859(3)	1.955(5)

Indeed, we observe what should be expected: since the rescattering diagram is not as sensitive to the core of the deuteron, using the OPE wave function in place of the standard one has only a small effect.

APPENDIX D: EFFECT OF THE δ TERMS: $\mathcal{O}^a_{2B}$ DIAGRAM

In this section we calculate the correction terms to the first two-body DW amplitude [Eq. (43)] which is shown in Fig. 9(a). Assuming that the δ truly are small compared to Eq. (45), we will only worry about calculating them one at a time, numbering the contribution of the δ from right to left as 1, 2, and 3. Note that we will display the results as calculated using the OPE deuteron and the Av18 initial state.

1. First $\mathcal{O}^a_{2B}$ correction term: $\Delta\mathcal{O}_1$

Consider the rightmost δ in Eq. (43),

$$\begin{aligned} \Delta\mathcal{O}_1 = {} & -\frac{\boldsymbol{\sigma}_1\cdot(\mathbf{p}-\mathbf{k})\boldsymbol{\sigma}_2\cdot(\mathbf{k}-\mathbf{p})}{-(\mathbf{p}-\mathbf{k})^2-\mu^2}F_{\pi NN}^2[(\mathbf{p}-\mathbf{k})^2]\frac{1}{-m_\pi} \\ & \times \frac{\frac{\mathbf{p}^2}{2m_N} - \frac{m_\pi}{2} + \frac{\gamma}{2}}{\sqrt{(\mathbf{p}-\mathbf{p}_i)^2+m_\pi^2}+\frac{\mathbf{p}^2}{2m_N}-\frac{m_\pi}{2}+\frac{\gamma}{2}}\mathbf{S}\cdot\mathbf{p}, \end{aligned} \tag{D1}$$

where $\mu^2 = 3m_\pi^2/4$ and $F_{\pi NN}$ is the form factor described in Appendix C. The easiest way to evaluate the matrix element of this operator is to let the OPE act to the left on the deuteron in position space. The resulting expression is then transformed to momentum space. We can expand the fraction in the integrand of Eq. (D1) into spherical harmonics (taking $\hat{\mathbf{p}}_i = \hat{\mathbf{z}}$),

$$\frac{\frac{\mathbf{p}^2}{2m_N} - \frac{m_\pi}{2} + \frac{\gamma}{2}}{\sqrt{(\mathbf{p}-\mathbf{p}_i)^2+m_\pi^2}+\frac{\mathbf{p}^2}{2m_N}-\frac{m_\pi}{2}+\frac{\gamma}{2}} = \sum_l A_l(p)Y_{l,0}(\hat{\mathbf{p}}), \tag{D2}$$

TABLE VI. Effect of using OPE deuteron on rescattering diagram.

Deuteron	Av18	Reid '93	Nijm II
Phenomenological	67.8	69.7	71.1
OPE ($n = 5$)	69.8	72.1	74.0

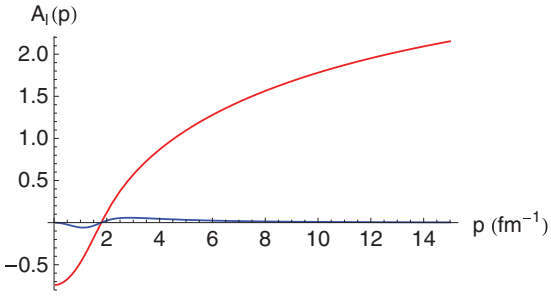

FIG. 11. (Color online) Coefficients of the expansion in Eq. (D2). The red curve shows $l = 0$ and the blue shows $l = 2$.

and note that only the $l = 0, 2$ terms will contribute to s-wave production. The expansion coefficients are shown in Fig. 11. Clearly the $l = 2$ term is small and we neglect it here to avoid the extra algebra involved with a $J = 2$ operator (resulting in the A_2 reduced matrix elements in the notation of Ref. [8]). We find

$$\frac{\Delta\mathcal{M}_1}{\mathcal{M}} = -34\%. \tag{D3}$$

2. Second $\mathcal{O}^a_{2B}$ correction term: $\Delta\mathcal{O}_2$

Next consider the term

$$\Delta\mathcal{O}_2 = \frac{\boldsymbol{\sigma}_1\cdot(\mathbf{p}-\mathbf{k})\boldsymbol{\sigma}_2\cdot(\mathbf{k}-\mathbf{p})}{-(\mathbf{p}-\mathbf{k})^2-\mu^2}F^2_{\pi NN}[(\mathbf{p}-\mathbf{k})^2] \times\frac{1}{\sqrt{(\mathbf{p}-\mathbf{k})^2+m_\pi^2}}\frac{1}{-m_\pi} \times\left(\frac{\mathbf{p}^2}{2m_N}-\frac{m_\pi}{2}+\frac{\gamma}{2}\right)\mathbf{S}\cdot\mathbf{p}. \tag{D4}$$

This term has a modified OPE,

$$\int\frac{d^3q}{(2\pi)^3}e^{-i\mathbf{q}\cdot\mathbf{r}}\frac{\boldsymbol{\sigma}_1\cdot\mathbf{q}\,\boldsymbol{\sigma}_2\cdot(-\mathbf{q})}{\mathbf{q}^2+\mu^2}F^2_{\pi NN}(\mathbf{q}^2)\frac{1}{\sqrt{\mathbf{q}^2+m_\pi^2}} \tag{D5}$$

$$\equiv\boldsymbol{\sigma}_1\cdot\nabla\boldsymbol{\sigma}_2\cdot\nabla\frac{\zeta(r)}{4\pi} \tag{D6}$$

$$=\frac{\mu^2}{12\pi}[S_{12}T_\zeta(r)+\boldsymbol{\sigma}_1\cdot\boldsymbol{\sigma}_2Y_\zeta(r)]. \tag{D7}$$

In Fig. 12 we compare the functions $T_\zeta(r)$ and $Y_\zeta(r)$ to traditional OPE which has μ in place of the square root in Eq. (D5). We use the Schrödinger equation to replace the $\mathbf{p}^2/2m_N$ with $V(r)$ and evaluate the matrix element in position space to find

$$\frac{\Delta\mathcal{M}_2}{\mathcal{M}} = +50\%. \tag{D8}$$

3. Third $\mathcal{O}^a_{2B}$ correction term: $\Delta\mathcal{O}_3$

Calculating the effects of the δ in the denominator of the OPE is difficult to do exactly due to the combination of momenta that appear,

$$\Delta\mathcal{O}_3 = \frac{\boldsymbol{\sigma}_1\cdot(\mathbf{p}-\mathbf{k})\boldsymbol{\sigma}_2\cdot(\mathbf{k}-\mathbf{p})}{-\left[\sqrt{(\mathbf{p}-\mathbf{k})^2+m_\pi^2}+\delta(\mathbf{p})\right]^2+m_\pi^2/4} \times F^2_{\pi NN}[(\mathbf{p}-\mathbf{k})^2]\frac{1}{-m_\pi}\mathbf{S}\cdot\mathbf{p} \tag{D9}$$

[recall that $\delta(\mathbf{p}) = \mathbf{p}^2/2m_N - m_\pi/2 + \gamma/2$]. Instead we will evaluate it for fixed values of δ which represent the deviation of $\mathbf{p}$ away from $\mathbf{p}_i$,

$$\delta_+ = \delta(p_i+m_\pi) = \frac{2p_im_\pi+m_\pi^2}{2m_N} = 0.45\,m_\pi, \tag{D10}$$

$$\delta_- = \delta(p_i-m_\pi) = \frac{-2p_im_\pi+m_\pi^2}{2m_N} = -0.32\,m_\pi. \tag{D11}$$

The modified tensor and central functions T_ξ and Y_ξ are shown in Fig 13.

We define the correction as

$$\Delta\mathcal{M}_3(\delta) = \mathcal{M}(\delta)-\mathcal{M}(0). \tag{D12}$$

We find

$$\frac{\Delta\mathcal{M}_3(\delta_+)}{\mathcal{M}} = +16\%, \tag{D13}$$

$$\frac{\Delta\mathcal{M}_3(\delta_-)}{\mathcal{M}} = -32\%. \tag{D14}$$

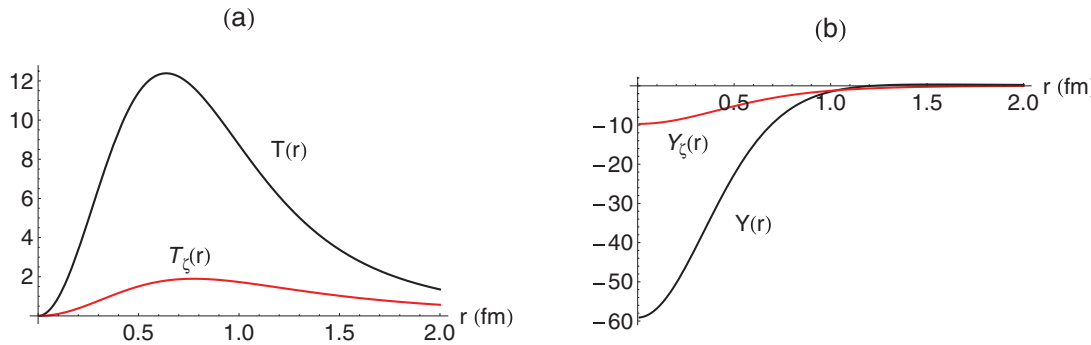

FIG. 12. (Color online) Effect of the square root on the OPE (a) tensor and (b) central radial functions.

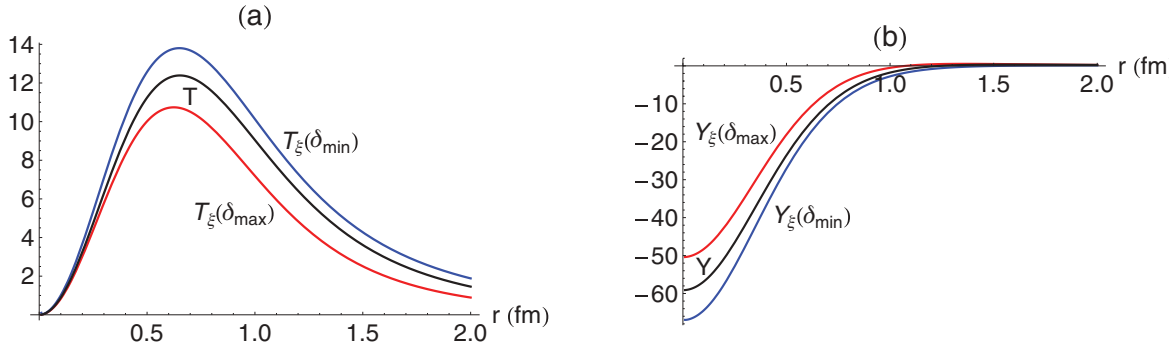

FIG. 13. (Color online) Effect of the δ on the OPE (a) tensor and (b) central radial functions.

4. Summary of $\mathcal{O}^a_{\rm 2B}$ corrections

For the purposes of estimating the net result we take the average of the estimates in Appendix D3 and find

$$\frac{\Delta\mathcal{M}_{\rm tot}}{\mathcal{M}} \approx -34\% + 50\% - 8\% = +8\%. \tag{D15}$$

We have successfully shown that the corrections to the first two-body DW amplitude are small, and actually *increase* the amplitude which is already twice as large as the traditional impulse approximation.

APPENDIX E: EFFECT OF THE δ TERMS: $\mathcal{O}^b_{\rm 2B}$ DIAGRAM

The second two-body DW amplitude's corrections are evaluated exactly as in the previous sub-sections and we just display the results here,

$$\frac{\Delta\mathcal{M}_1}{\mathcal{M}} = -35\%, \tag{E1}$$

$$\frac{\Delta\mathcal{M}_2}{\mathcal{M}} = -39\%, \tag{E2}$$

$$\frac{\Delta\mathcal{M}_3(\delta_+)}{\mathcal{M}} = \frac{\Delta\mathcal{M}_3(\delta_-)}{\mathcal{M}} = +3\%, \tag{E3}$$

with the net result

$$\frac{\Delta\mathcal{M}_{\rm tot}}{\mathcal{M}} \approx -35\% - 39\% + 3\% = -71\%. \tag{E4}$$

We see that the corrections to the approximation in Eq. (46) are fairly large, but this has a negligible effect because the amplitude is already small compared to the first two-body DW amplitude.

APPENDIX F: HEAVY MESON EXCHANGE

Consider the loop on the left-hand side of Fig. 14 which is obtained by using OPE for the left K in Eq. (33) and σ exchange (the dominant intermediate-range mechanism) for the right K. Note that this loop only differs from Fig. 6 in two ways: the meson-nucleon vertex (here we consider only scalar isoscalar) and the meson mass. We use a typical set of parameters [33], $g_\sigma^2/4\pi = 7.1$ and $m_\sigma = 550$ MeV.

The result of integrating over energy will proceed exactly as it did with the pion resulting in the two diagrams shown on the RHS of Fig. 14. To interpret the $I^{\sigma,a}_{\rm 2B}$ term (again, neglecting stretched box diagrams), we absorb the sigma exchange into the initial state and no new term is added. However, in the $I^{\sigma,b}_{\rm 2B}$ term, after absorbing the pion exchange into the final state, we are left with a new operator. The amplitude for this operator can be obtained from that of Fig. 9(b) with the following change:

$$\left(\frac{g_A}{2f_\pi}\right)^2 \frac{\mu^3}{3}\left[2\left(1+\frac{3}{\mu r}+\frac{3}{(\mu r)^2}\right)+1\right]\frac{e^{-\mu r}}{\mu r}$$
$$\to\ g_\sigma^2 \mu_\sigma \frac{e^{-\mu_\sigma r}}{\mu_\sigma r}, \tag{F1}$$

where $\mu^2 = 3m_\pi^2/4$ and $\mu_\sigma^2 = m_\sigma^2 - (m_\pi/2)^2$. We find

$$A^{\sigma,b}_{\rm 2B} = -7.24, \tag{F2}$$

which is larger in magnitude than the pionic $A^{{\rm DW},b}_{\rm 2B}$ (with the same sign) but smaller than $A^{{\rm DW},a}_{\rm 2B}$ (with the opposite sign). Since m_σ is relatively large, we can safely ignore the two δ corrections that are competing with ω_i and only need to evaluate

$$\frac{\Delta\mathcal{M}_1}{\mathcal{M}} = -27\%. \tag{F3}$$

One natural question is whether the static σ exchange already present in the initial-state wave function is a sufficient approximation for the contribution considered in this section. To answer this question, we can evaluate the traditional impulse approximation with

$$|\Psi\rangle_i^\sigma = |p_1, p_2\rangle + GV_\sigma|\Psi\rangle_i, \tag{F4}$$

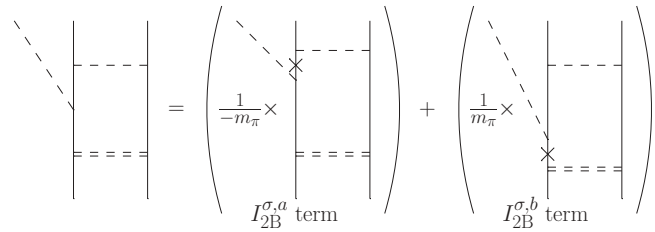

FIG. 14. Impulse approximation with distorted waves: initial state heavy meson exchange. Solid lines represent nucleons, dashed lines pions, and the double solid line a σ meson. Crosses represent propagators which are absent due to the partial fractions decomposition.

where here we employ a static σ exchange that is present (at least effectively) in the wave function. Using this initial-state wave function, we calculate

$$\mathcal{M}^{\sigma}_{\mathrm{1B}} = {}_f\langle\phi|\mathcal{O}_\pi|\Psi\rangle^{\sigma}_i, \tag{F5}$$

and find the reduced matrix element,

$$A^{\sigma}_{\mathrm{1B}} = -3.3. \tag{F6}$$

Thus we see that the σ exchange in the traditional impulse approximation is an underestimate (in magnitude) of the true nonstatic exchange dictated by the loop integral.

Of course there is no σ in traditional BχPT, so this section is simply telling us that to achieve high accuracy it is indeed important to use more than just simple pion exchange when forming the original box diagram. Such a calculation is beyond the scope of this work.

[1] S. Weinberg, Physica A **96**, 327 (1979).
[2] J. Gasser and H. Leutwyler, Ann. Phys. **158**, 142 (1984).
[3] V. Bernard, N. Kaiser, and U. G. Meissner, Z. Phys. C **60**, 111 (1993).
[4] E. Epelbaum, W. Glockle, and U.-G. Meissner, Nucl. Phys. A **747**, 362 (2005).
[5] D. R. Entem and R. Machleidt, Phys. Rev. C **68**, 041001 (2003).
[6] S. K. Bogner, T. T. S. Kuo, and A. Schwenk, Phys. Rep. **386**, 1 (2003).
[7] V. Baru, E. Epelbaum J. Haidenbauer, C. Hanhart, A. E. Kudryavtsev, V. Lensky, and U. G. Meissner, Phys. Rev. C **80**, 044003 (2009).
[8] D. R. Bolton and G. A. Miller, Phys. Rev. C **81**, 014001 (2010).
[9] A. Filin *et al.*, Phys. Lett. B **681**, 423 (2009).
[10] T. D. Cohen, J. L. Friar, G. A. Miller, and U. van Kolck, Phys. Rev. C **53**, 2661 (1996).
[11] C. Hanhart, Phys. Rept. **397**, 155 (2004).
[12] D. S. Koltun and A. Reitan, Phys. Rev. **141**, 1413 (1966).
[13] D. R. Bolton and G. A. Miller, Phys. Rev. C **82**, 024001 (2010).
[14] A. Gardestig, D. R. Phillips, and C. Elster, Phys. Rev. C **73**, 024002 (2006).
[15] S. R. Beane and M. J. Savage, Nucl. Phys. A **713**, 148 (2003).
[16] A. Bulgac, G. A. Miller, and M. Strikman, Phys. Rev. C **56**, 3307 (1997).
[17] M. H. Partovi and E. L. Lomon, Phys. Rev. D **2**, 1999 (1970).
[18] G. A. Miller and B. C. Tiburzi, Phys. Rev. C **81**, 035201 (2010).
[19] E. E. Jenkins and A. V. Manohar, Phys. Lett. B **255**, 558 (1991).
[20] S. Scherer, Adv. Nucl. Phys. **27**, 277 (2003).
[21] C. J. Horowitz, Phys. Rev. C **48**, 2920 (1993).
[22] T. S. H. Lee and D. O. Riska, Phys. Rev. Lett. **70**, 2237 (1993).
[23] R. B. Wiringa, V. G. J. Stoks, and R. Schiavilla, Phys. Rev. C **51**, 38 (1995).
[24] V. Lensky *et al.*, Eur. Phys. J. A **27**, 37 (2006).
[25] C. Hanhart and V. Baru (private communications, 2010).
[26] J. L. Friar, B. F. Gibson, and G. L. Payne, Phys. Rev. C **30**, 1084 (1984).
[27] C. Hanhart, G. A. Miller, F. Myhrer, T. Sato, and U. van Kolck, Phys. Rev. C **63**, 044002 (2001).
[28] V. G. J. Stoks, R. A. M. Klomp, C. P. F. Terheggen, and J. J. de Swart, Phys. Rev. C **49**, 2950 (1994).
[29] D. A. Hutcheon *et al.*, Phys. Rev. Lett. **64**, 176 (1990).
[30] P. Heimberg *et al.*, Phys. Rev. Lett. **77**, 1012 (1996).
[31] M. Drochner *et al.* (GEM Collaboration), Nucl. Phys. A **643**, 55 (1998).
[32] T. Strauch *et al.*, Phys. Rev. Lett. **104**, 142503 (2010).
[33] T. E. O. Ericson and W. Weise, Pions and Nuclei, Vol. 74 of *The International Series of Monographs on Physics* (Clarendon, Oxford, 1988).